cmgh
CELLULAR AND MOLECULAR GASTROENTEROLOGY AND HEPATOLOGY

ORIGINAL RESEARCH

LLGL1 Regulates Gemcitabine Resistance by Modulating the ERK-SP1-OSMR Pathway in Pancreatic Ductal Adenocarcinoma

Yin-Xin Zhu,[1,*] Chi Han Li,[1,*] Guolin Li,[2,§] Huiyi Feng,[1,§] Tian Xia,[1] Chi Hin Wong,[1] Frederic Khe Cheong Fung,[1] Joanna Hung-Man Tong,[3] Ka-Fai To,[3] Rufu Chen,[5] and Yangchao Chen[1,4]

[1]School of Biomedical Sciences, Faculty of Medicine, [3]Department of Anatomical and Cellular Pathology, Prince of Wales Hospital, The Chinese University of Hong Kong, Shatin, Hong Kong; [2]Department of Hepatobiliary Surgery, Sun Yat-sen Memorial Hospital, Guangzhou, China; [4]Shenzhen Research Institute, The Chinese University of Hong Kong, Shenzhen, China; [5]Guangdong Provincial People's Hospital, Guangzhou, Guangdong Province, China

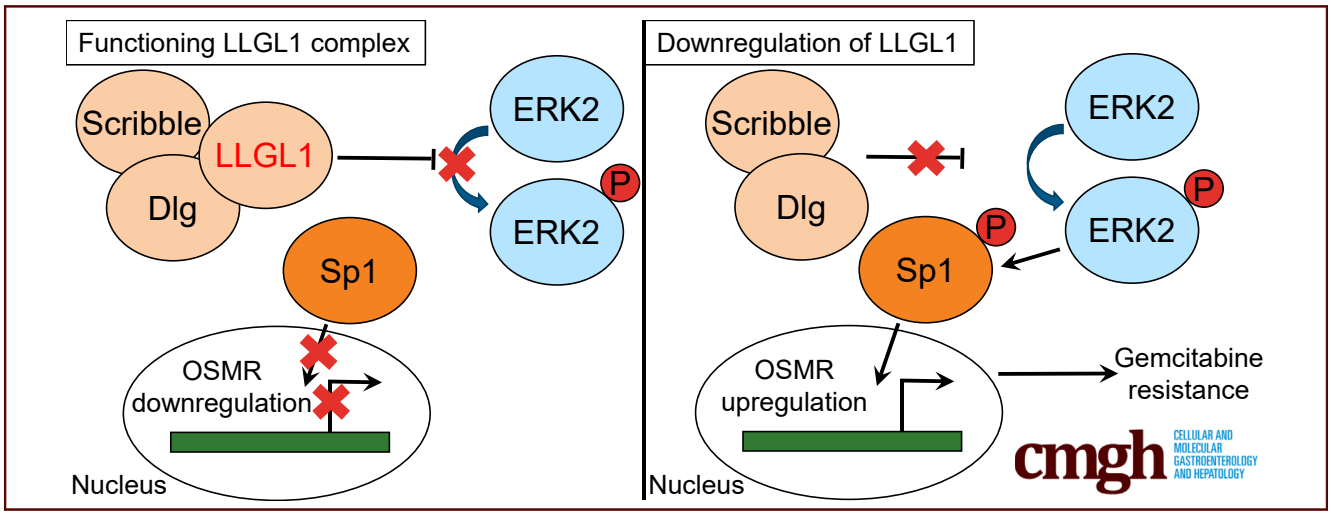

SUMMARY

Shorter survival has been observed in patients with tumor expressing a low lethal giant larvae homolog 1 (LLGL1) level. LLGL1 markedly reduced the gemcitabine chemosensitivity by repressing oncostatin M receptor expression in pancreatic ductal adenocarcinoma cells. LLGL1 regulated gemcitabine resistance through the extracellular signal-regulated kinase 2–specificity protein 1–oncostatin M receptor pathway.

BACKGROUND & AIMS: Gemcitabine resistance is rapidly acquired by pancreatic ductal adenocarcinoma (PDAC) patients. Novel approaches that predict the gemcitabine response of patients and enhance gemcitabine chemosensitivity are important to improve patient survival. We aimed to identify genes as novel biomarkers to predict the gemcitabine response and the therapeutic targets to attenuate chemoresistance in PDAC cells.

METHODS: Genome-wide RNA interference screening was conducted to identify genes that regulated gemcitabine chemoresistance. A cell proliferation assay and a tumor formation assay were conducted to study the role of lethal giant larvae homolog 1 (LLGL1) in gemcitabine chemoresistance. Levels of LLGL1 and its regulating targets were measured by immunohistochemical staining in tumor tissues obtained from patients who received gemcitabine as a single therapeutic agent. A gene-expression microarray was conducted to identify the targets regulated by LLGL1.

RESULTS: Silencing of LLGL1 markedly reduced the gemcitabine chemosensitivity in PDAC cells. Patients had significantly shorter survival (6 months) if they bore tumors expressing low LLGL1 level than tumors with high LLGL1 level (20 months) (hazard ratio, 0.1567; 95% CI, 0.05966–0.4117). Loss of LLGL1 promoted cytokine receptor oncostatin M receptor (OSMR) expression in PDAC cells that led to gemcitabine resistance, while knockdown of OSMR effectively rescued the chemoresistance phenotype. The LLGL1-OSMR regulatory pathway showed great clinical importance because low LLGL1 and high OSMR expressions were observed frequently in PDAC tissues. Silencing of LLGL1 induced phosphorylation of extracellular signal-regulated kinase 2 and specificity protein 1 (Sp1), promoted Sp1 (pThr453) binding at the OSMR promoter, and enhanced OSMR transcription.

CONCLUSIONS: LLGL1 possessed a tumor-suppressor role as an inhibitor of chemoresistance by regulating OSMR–extracellular signal-regulated kinase 2/Sp1 signaling. The data sets generated and analyzed during the current study are available in the Gene Expression Omnibus repository (ID: GSE64681). *(Cell Mol Gastroenterol Hepatol 2020;10:811–828; https://doi.org/10.1016/j.jcmgh.2020.06.009)*

Keywords: Pancreatic Cancer; Gemcitabine; Oncostatin M Receptor; SP1 Signaling.

Pancreatic ductal adenocarcinoma (PDAC) accounts for 95% of exocrine pancreatic cancer. It remains one of the most lethal malignancies, with a 5-year survival rate of less than 9%.[1] Most PDAC cases are already at advanced stages at the time of diagnosis, missing the chances of curative surgical resection.[2] Chemotherapy only benefits a minority of PDAC patients, mainly because of the innate and easily acquired chemoresistance from cancer cells to the first-line chemotherapeutic drug gemcitabine.[3] Diverse cellular functions including nucleoside transport, metabolism, proliferation, apoptosis, cancer stemness, and epithelial-mesenchymal transition (EMT) contribute to gemcitabine resistance. Numerous genes involved in these functions such as *CD44, ABCB1, S100A4, S100P, COX2,* E-cadherin, and *ZEB-1*[4–8] were identified to regulate gemcitabine resistance. However, there is still a lack of effective biomarkers to predict the response of patients to gemcitabine treatment. Accurate prediction of gemcitabine response could aid in the development of therapeutic strategies against gemcitabine resistance.

In this study, we attempted to identify the candidate genes that were capable of sensitizing PDAC cells to gemcitabine as well as predicting the gemcitabine response of patients. We adapted a RNA interference (RNAi) screening approach to achieve genome-wide gene knockdown, and then select the PDAC cells that acquired resistance to gemcitabine. Subsequently, we identified a mammalian homolog of lethal giant larvae (Lgl) as a potential gemcitabine-sensitizing gene. Lgl is an evolutionarily conserved WD40 domain-containing protein that functions to maintain cell polarity.[9,10] Lgl is one of the core components of the Scribble complex in drosophila that is involved in the regulation of intracellular and intercellular signaling. Mammalian genomes contain 2 Lgl homologs, lethal giant larvae homolog 1 and 2 (*LLGL1* and *LLGL2*).[11,12] Reduced expression of LLGL1 has been detected in various malignancies[13–15] including PDAC,[16] and loss of LLGL1 indicated a poor survival rate in PDAC patients.[16] A study also illustrated that overexpression of LLGL1 induced apoptosis in esophageal carcinoma cells.[17] Currently, there is no study reporting any role of LLGL1 with gemcitabine resistance. Characterization of the role of LLGL1 in regulating gemcitabine response in PDAC cells could prompt the development of novel therapeutic strategies against gemcitabine resistance.

Results

Genome-Wide RNAi Screening Identified LLGL1 as a Gemcitabine-Sensitizing Gene

The workflow of the genome-wide RNAi screening is shown in Figure 1*A*. In detail, we first transduced the Capan2 cells with small interfering RNA (siRNA) library lentivirus for the identification of genes that regulated gemcitabine resistance. Capan2 was selected as the cell line model because the cells were reported to be sensitive to gemcitabine treatment.[18] In theory, cells would gain gemcitabine resistance when the genes critical in regulating gemcitabine response were knocked-down. The gemcitabine-resistant cells could expand and the respective siRNAs effectors were enriched in the whole cell population. In turn, total RNAs were extracted from the treatment and control cells for complementary DNA (cDNA) conversion. siRNA effectors in the cDNA samples were amplified and were subjected to microarray analysis to measure the abundance of the residue siRNA effectors. By comparing the abundance of the siRNA effectors between the treatment and control groups, we could identify the genes that were associated with gemcitabine response. siRNA effectors that were increased by 3-fold or more in the treatment group were considered to be capable of generating gemcitabine resistance in PDAC cells (Figure 1*A*). Among them, *GNPAT* and *PTPN2* were associated with the enhancement of chemosensitivity in cancer cells,[19,20] which proved the concept of our screening method in identifying chemoresistance-associated genes.

Literature reviews have suggested that ring finger protein 126, glutamate ionotropic receptor kainate type subunit 2, LLGL1, and erythropoietin receptor were associated with cancer development, but their roles in gemcitabine resistance were unclear. We then inhibited their levels by transfecting siRNAs in Capan2 cells (Figure 1*B*, upper panel). A cell toxicity assay showed that only the inhibition of LLGL1 could significantly hinder the effectiveness of gemcitabine at various concentrations in Capan2 cells, whereas inhibiting the other genes failed to promote gemcitabine resistance (Figure 1*B*, lower panel, and *C*). A previous study showed that Capan2 was sensitive to gemcitabine treatment, but gemcitabine resistance was observed in PANC1 cells because a much higher gemcitabine dose was needed to cause 50% of cell death.[18] We then measured the expression level of LLGL1 in a panel of PDAC cell lines. The profiling of LLGL1 expression in human pancreatic ductal epithelial (HPDE) and PDAC cell lines showed that its expression was higher in HPDE and gemcitabine-sensitive Capan2 and SW1990 cells than in gemcitabine-resistant PANC1 cells[18] (Figure 1*D*). It showed that low endogenous LLGL1 level could contribute to the gemcitabine resistance phenotype in the cell line. Therefore, we hypothesized that LLGL1 was a gene to mediate the sensitivity of PDAC cells to gemcitabine.

To analyze the relationship between LLGL1 expression in tumors and disease-free survival, we first measured the

*Authors contributed equally; §Authors contributed equally.

Abbreviations used in this paper: cDNA, complementary DNA; ChIP, chromatin immunoprecipitation; CSC, cancer stem cell; Dlg, discs large protein; EMT, epithelial-mesenchymal transition; ERK2, extracellular signal-regulated kinase 2; hENT1, human equilibrative nucleoside transporter 1; HPDE, human pancreatic ductal epithelial; IC50, median inhibitory concentration; IHC, immunohistochemistry; Lgl, lethal giant larvae; LLGL1, lethal giant larvae homolog 1; MTT, 3-(4,5-dimethylthiazol-2-yl)-2,5-diphenyltetrazolium bromide; OSM, oncostatin M; OSMR, oncostatin M receptor; PDAC, pancreatic ductal adenocarcinoma; Pol II, RNA polymerase II; qRT-PCR, quantitative reverse-transcription polymerase chain reaction; RNAi, RNA interference; siLLGL1, small interfering lethal giant larvae homolog 1; siRNA, small interfering RNA; Sp1, specificity protein 1; SWH, Salvador/Warts/Hippo; TGF, transforming growth factor.

Most current article

2352-345X
https://doi.org/10.1016/j.jcmgh.2020.06.009

expression level of LLGL1 by immunohistochemical (IHC) staining in the tumor tissues of 29 PDAC patients collected from Sun Yat-sen Memorial Hospital. These patients received gemcitabine as the single agent in adjuvant chemotherapy. Among them, 13 patients had LLGL1-positive tumors and 16 patients had LLGL1-negative tumors (Figure 1*E*). Patients with LLGL1-positive tumors had significantly longer disease-free survivals compared with patients with negative tumors ($P < .001$), because their median disease-free survival was 20 months and 6 months, respectively (hazard ratio, 0.1567; 95% CI, 0.05966–0.4117) (Figure 1*F*, Table 1). Taken together, we showed that LLGL1 level was associated with the gemcitabine resistance phenotype in human PDAC.

LLGL1 Was a Tumor Suppressor That Regulated Gemcitabine Response in PDAC Cells

LLGL1 has been identified as a tumor suppressor in multiple cancer types,[13,14] but its role in PDAC is unclear. We observed that LLGL1 expression was reduced significantly in human PDAC tissues compared with adjacent nontumor tissues (Figure 2*A*, Table 2), which is consistent with a previous report.[16] We then studied the effect of LLGL1 down-regulation in regulating gemcitabine resistance in PDAC cells. We transduced lentivirus to inhibit LLGL1 in Capan2 and SW1990 cells (Figure 2*B*) by short hairpin RNAs. A drug cytotoxicity assay showed that knockdown of LLGL1 significantly reduced the gemcitabine response, which resulted in more than an approximately 24- and an approximately 11-fold increase of the median inhibitory concentration (IC50) in CAPAN2 and SW1990 cells, respectively (IC50 from 0.1048 ± 0.0883 μmol/L to 2.7293 ± 0.7333 μmol/L in Capan2 cells and from 0.0234 ± 0.0311 μmol/L to 0.2660 ± 0.1265 μmol/L in SW1990 cells) (Figure 2*B*). Subsequently, we attempted to study the tumor-suppressor role of LLGL1 in PDAC cells. A colony formation assay was performed in the LLGL1-inhibited PDAC cells, and showed that knockdown of LLGL1 led to increases of colonies in both CAPAN2 and SW1990 cells (Figure 2*C*). In addition, a soft agar assay was performed to study the role of LLGL1 in the transformation ability of the PDAC cells. It showed that knockdown of LLGL1 could increase the number of colonies formed in the soft agar for both PDAC cell lines (Figure 2*D*).

To further validate the function of LLGL1 in colony-forming abilities, we overexpressed LLGL1 in Panc1 cells in which it had a low level of endogenous LLGL1. Full-length LLGL1 cDNA was cloned into a lentiviral vector, and the vector was used to package lentivirus. After transducing Panc1 cells with the LLGL1-overexpressing lentivirus, colony formation and soft agar assay were performed. We showed that the numbers of colonies formed by Panc1 cells in both assays largely were reduced upon overexpression of LLGL1 (Figure 2*E*). Taken together, we showed that the inhibition of LLGL1 could promote resistance to gemcitabine treatment, cell growth, and transforming ability in PDAC cells.

To study the mechanism of LLGL1 in regulating gemcitabine resistance, we first studied the potential association between LLGL1 the multidrug resistance phenotype by performing a Rhodamine 123 accumulation and efflux assay.[21] However, knockdown of LLGL1 in gemcitabine-treated or untreated Capan2 cells only slightly reduced Rhodamine 123 accumulation (Figure 2*F*), and had almost no effect on the efflux efficiency of Rhodamine 123 (Figure 2*G* and *H*). Thus, the induction of gemcitabine resistance by LLGL1 depletion was independent of the multidrug resistance phenotype that led to active gemcitabine efflux.

Oncostatin M Receptor Was the Major Downstream Target of LLGL1 That Mediated Gemcitabine Resistance in PDAC Cells

To elucidate the mechanisms underlying the regulation of gemcitabine response by LLGL1 in PDAC cells, we attempted to identify LLGL1 regulating targets through gene expression microarray (Figure 3*A*). Genome-wide microarray analysis was conducted in cells with knockdown of LLGL1. Gene Ontology analysis showed that a large proportion of genes with 2-fold or more differentiated expression fell into the categories of cell proliferation, which was consistent with the tumor-suppressive role of LLGL1. We validated several candidate genes including oncostatin M receptor (OSMR), interleukin 6, transforming growth factor (TGF)β1, TGFβ2, and bone morphogenetic protein 6, which participated in important signaling pathways mediating gemcitabine resistance and had their expression levels changed by more than 2-fold after inhibition of LLGL1 (Figure 3*B*). Knockdown of LLGL1 significantly increased the expression of OSMR in Capan2 and SW1990 cells (Figure 3*C*). Importantly, only inhibition of OSMR expression effectively reversed gemcitabine resistance in LLGL1-inhibited Capan2 (Figure 3*D*, upper panel) and SW1990 cells (Figure 3*D*, lower panel). Western blot and quantitative reverse-transcription polymerase chain reaction (qRT-PCR) analysis showed that OSMR expression was markedly higher in PDAC cells compared with HPDE cells (Figure 3*E*). In turn, we would like to study the role of LLGL1 to OSMR promoter activity. A luciferase assay showed that OSMR promoter induced proper promoter activity in HEK293 cells. More importantly, knockdown of LLGL1 significantly increased luciferase activity of reporter containing OSMR promoter in Capan2 and SW1990 cells (Figure 3*F*), suggesting that LLGL1 regulated the expression of OSMR through modulating its promoter activity. Although LLGL1 regulated the expression of signal transducer and activator of transcription 3, transforming growth factor beta receptor I and II, we showed that they did not participate in the modulation of gemcitabine resistance in PDAC cells (Figure 3*G*). Therefore, we showed that up-regulation of OSMR may contribute to the gemcitabine resistance mediated by LLGL1. We also showed that LLGL1 could regulate OSMR expression by inhibiting the promoter activity of OSMR.

To understand the mechanism of LLGL1-regulated gemcitabine resistance, we attempted to observe the change of drug resistance–associated genes from the microarray data. We excluded any possible role of LLGL1 in

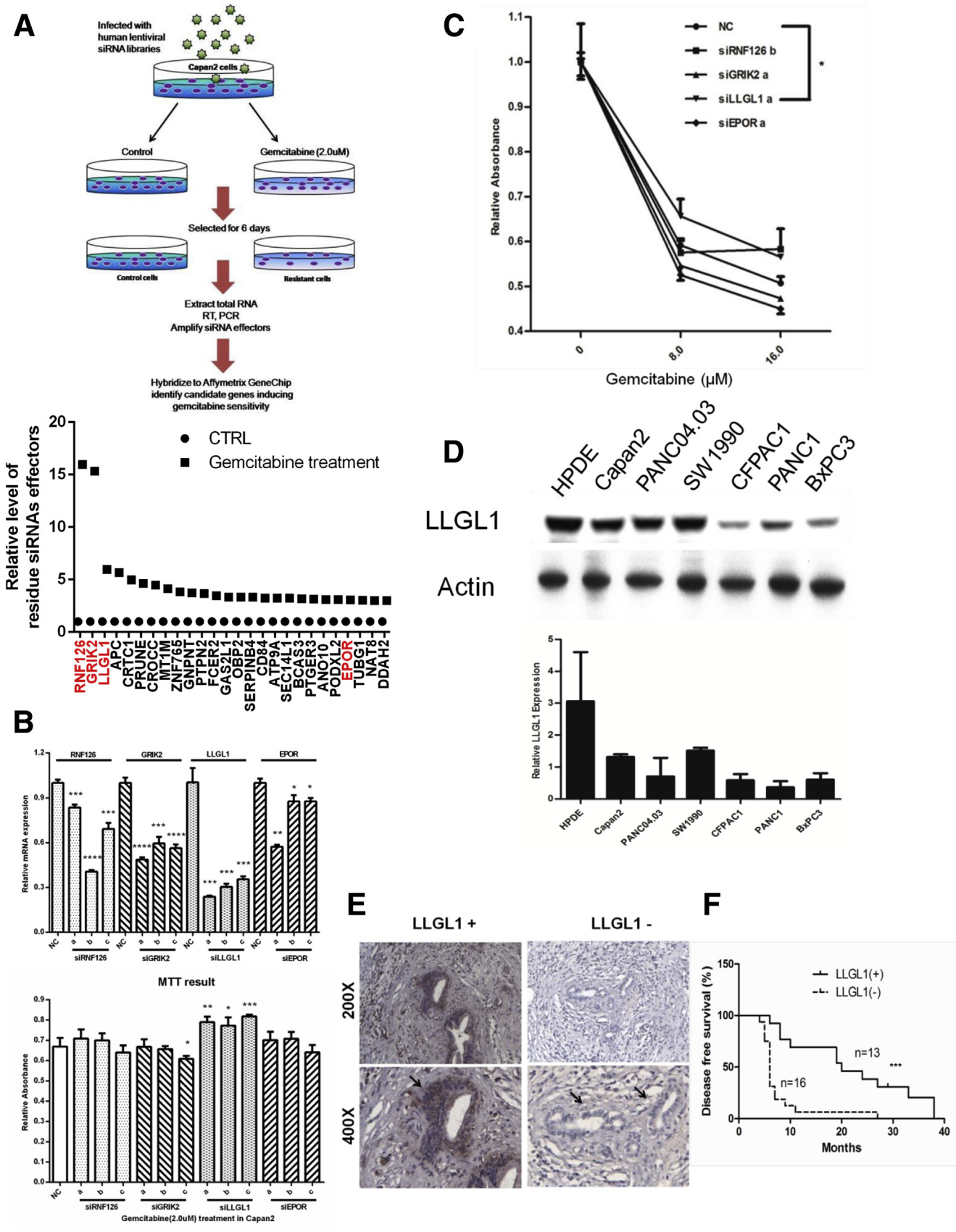
A
Infected with human lentiviral siRNA libraries
Capan2 cells
Control
Gemcitabine (2.0uM)
Selected for 6 days
Control cells
Resistant cells
Extract total RNA
RT, PCR
Amplify siRNA effectors
Hybridize to Affymetrix GeneChip identify candidate genes inducing gemcitabine sensitivity
Relative level of residue siRNAs effectors
CTRL
Gemcitabine treatment
RNF126 GRIK2 LLGL1 APC CRTC1 PRUNE CROCC MT1M ZNF765 GNPNT PTPN2 FCER2 GAS2L1 OBP2 SERPINB4 CD84 ATP9A SEC14L1 BCAS3 PTGER3 ANO10 PODXL2 EPOR TUBG1 NAT8 DDAH2
B
RNF126
GRIK2
LLGL1
EPOR
Relative mRNA expression
NC a b c
siRNF126
siGRIK2
siLLGL1
siEPOR
MTT result
Relative Absorbance
Gemcitabine(2.0uM) treatment in Capan2
C
NC
siRNF126 b
siGRIK2 a
siLLGL1 a
siEPOR a
Relative Absorbance
Gemcitabine (μM)
D
HPDE Capan2 PANC04.03 SW1990 CFPAC1 PANC1 BxPC3
LLGL1
Actin
Relative LLGL1 Expression
E
LLGL1 +
LLGL1 -
200X
400X
F
LLGL1(+)
LLGL1(-)
Disease free survival (%)
n=13
n=16
***
Months

Table 1. Clinical Pathologic Data of 29 PDAC Patients From Sun Yat-sen Memorial Hospital

	LLGL1 positive	LLGL1 negative	*P* value
Sex			
Male	7	9	.9907
Female	6	7	
Age, *y*			
20–30	2	0	.8187
31–40	0	0	
41–50	0	1	
51–60	6	7	
61–70	4	5	
71–80	1	3	
Pathologic types			
Ductal adenocarcinoma	12	15	.9960
Adenosquamous carcinoma	0	1	
Acinous cell carcinoma	1	0	
Differentiation degree			
Poor	0	4	.9178
Medium	9	11	
High	3	0	
Missing	1	1	
Diabetes			
Yes	0	4	.9923
No	13	12	
Hypertension			
Yes	3	5	.9973
No	10	11	
T stage			
T1	0	0	.9763
T2	2	1	
T3	9	11	
T4	2	4	
N stage			
N0	6	8	.6617
N1	7	8	
N2	0	0	
N3	0	0	
M stage			
M0	13	16	NS
M1	0	0	
Clinical stage			
I	2	1	.9750
II	9	11	
III	2	4	
IV	0	0	

regulating gemcitabine metabolism because the gene expression microarray indicated that candidate genes involved in the cellular uptake and metabolism of gemcitabine were not changed significantly after knockdown of LLGL1 in Capan2 cells (Figure 3*H*). Of note, qRT-PCR showed that the expression of human equilibrative nucleoside transporter (hENT)1 and hENT2, 2 major nucleoside transporters involved in cellular uptake of gemcitabine, were down-regulated significantly after inhibition of LLGL1 (Figure 3*I*). The cellular uptake of gemcitabine depends mainly on the activity of nucleoside transporters. Seven distinct nucleoside transporter activities on both sodium-independent, concentrative nucleoside transporter (CNT) manner already have been figured out in human cells, and, of them, hENT1 and hENT2 showed similar broad permeable selectivity for purine and pyrimidine nucleosides[22] and are widely distributed in different cell types. Therefore, hENT1 and hENT2 can be the major mediators of cellular gemcitabine uptake,[23] whose deficiency is expected to reduce cellular uptake of gemcitabine and mediate gemcitabine resistance. It has been suggested that LLGL1 potentially regulated the gemcitabine response by limiting cellular uptake of gemcitabine.

OSMR Expression Was Up-regulated Frequently and Correlated Negatively With LLGL1 in Human PDAC

The role of OSMR in PDAC has been largely unexplored. To study the role of OSMR in PDAC, we measured the OSMR expression level in human PDAC tissues by IHC staining. IHC staining in tissue microarray showed that OSMR expression was strongly increased in PDAC specimens in contrast to nontumor pancreatic ductal cells. Significantly increased OSMR expression was observed in grade I, grade II, and grade III PDAC tissues compared with normal pancreas. In contrast, down-regulation of LLGL1 expression was observed in grade II and grade III PDAC tissues (Figure 4*A* and *B*). The chi-square test and Pearson correlation showed that OSMR and LLGL1 were correlated negatively in PDAC tissues (Figure 4*B* and *C*). OSMR was reported to form a heterodimerized receptor with glycoprotein 130 and could be activated specifically by its ligand OSM. qRT-PCR showed that the expression of OSM was increased in PDAC cells and

Figure 1. (***See previous page***). **Genome-wide RNAi screening was performed in Capan2 cells and identified LLGL1 as a gemcitabine-sensitizing gene.** (*A*) Genome-wide RNAi screening for genes associated with gemcitabine response was performed according to the workflow. Relative levels of residue siRNA effectors were shown, which suggested they were candidate gemcitabine-sensitizing genes. Genes colored in red were selected for further validation. (*B*) *Upper*: Knockdown efficiency of siRNAs targeting RNF126, glutamate ionotropic receptor kainate type subunit 2, LLGL1, and erythropoietin receptor. *Lower*: Cells then were treated with 2 μmol/L gemcitabine after siRNA inhibition. Drug cytotoxicity assay showed that knockdown of LLGL1 by 3 different siRNAs could induce gemcitabine resistance in Capan2 cells. (*C*) Drug cytotoxicity assay showed that only knockdown of LLGL1 significantly reduced gemcitabine response at 8 and 16 μmol/L in Capan2 cells. (*D*) LLGL1 expression level profiling in HPDE and PDAC cells showed that LLGL1 levels in HPDE and gemcitabine-sensitive Capan2 and SW1990 cells were much higher than that in gemcitabine-resistant PANC1 cells. (*E*) IHC staining was performed to measure the LLGL1 level in 29 pairs of PDAC tumor and nontumor tissues, and (*F*) patients with LLGL1-positive tumors had significantly longer disease-free survivals when compared with those with LLGL1-negative tumors ($P < .001$). *$P < .05$, **$P < .01$, ***$P < .001$, and ****$P < .0001$. CTRL, control; EPOR, erythropoietin receptor; mRNA, messenger RNA; NC, negative control.

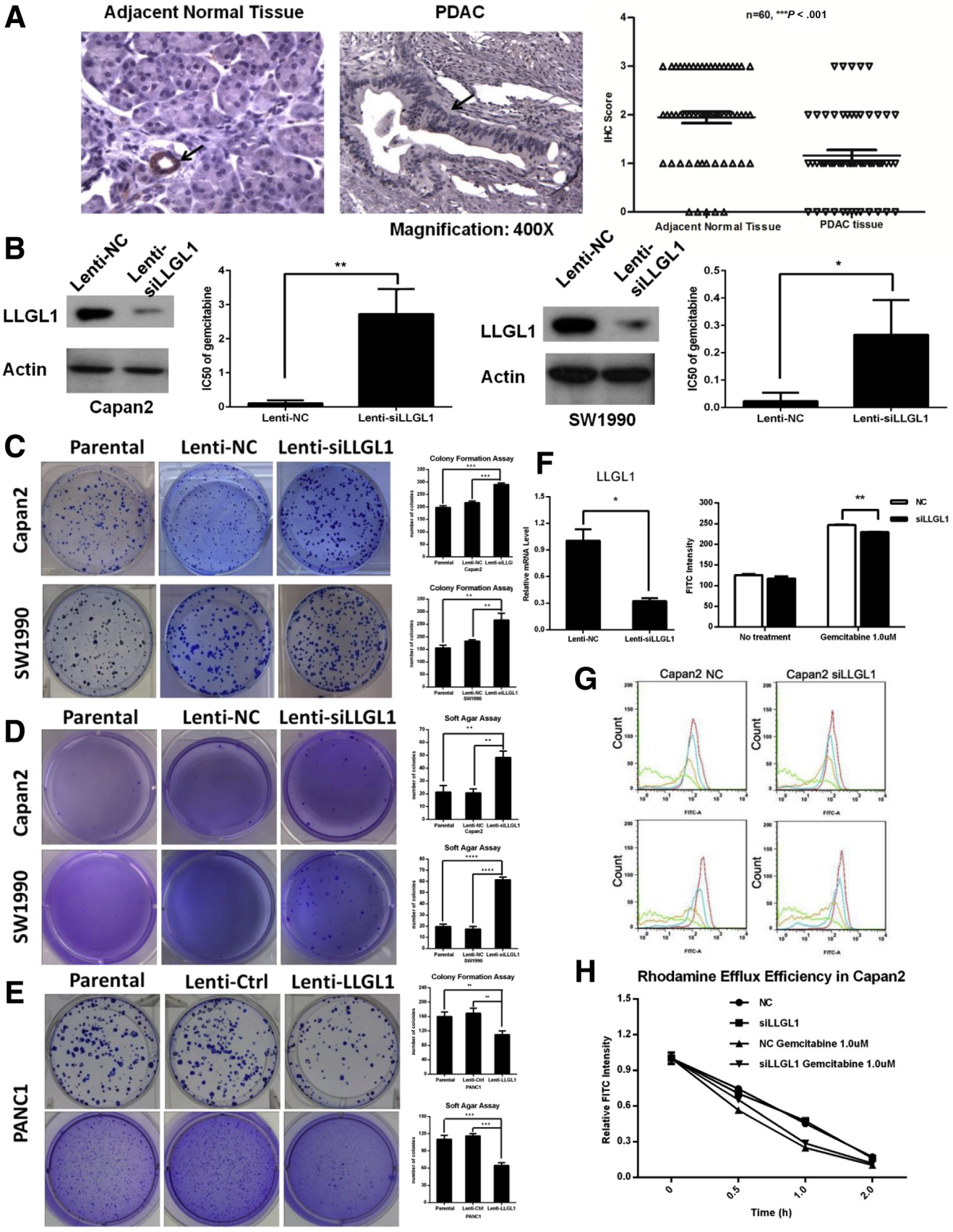
A
Adjacent Normal Tissue
PDAC
n=60, ***P < .001
IHC Score
Adjacent Normal Tissue
PDAC tissue
Magnification: 400X
B
Lenti-NC
Lenti-siLLGL1
LLGL1
Actin
Capan2
IC50 of gemcitabine
Lenti-NC
Lenti-siLLGL1
SW1990
C
Parental
Lenti-NC
Lenti-siLLGL1
Capan2
SW1990
Colony Formation Assay
D
Soft Agar Assay
E
Lenti-Ctrl
Lenti-LLGL1
PANC1
F
LLGL1
Relative mRNA Level
FITC Intensity
No treatment
Gemcitabine 1.0uM
NC
siLLGL1
G
Capan2 NC
Capan2 siLLGL1
Count
FITC-A
H
Rhodamine Efflux Efficiency in Capan2
NC
siLLGL1
NC Gemcitabine 1.0uM
siLLGL1 Gemcitabine 1.0uM
Relative FITC Intensity
Time (h)

Table 2. Clinical Pathologic Data of 60 PDAC Patients From Prince of Wales Hospital

N	60
Sex, n (%)	
Male	34 (56.7)
Female	26 (43.3)
Age, *y* (range)	45–79
Pathologic type, n (%)	
Well differentiated	8 (17.0)
Moderately differentiated	34 (72.3)
Poorly differentiated	5 (10.6)
Regional lymph node metastasis, n (%)	
No	28 (50.9)
Yes	27 (49.1)

tissues (Figure 4*D* and *E*). Therefore, OSMR signaling could be stimulated in PDAC cells by autocrine mode.

A recent study showed that activation of OSMR signaling was correlated strongly with the expression of multiple EMT and cancer stem cell (CSC) genes in pancreatic cancer.[24] Our microarray analysis indicated that several mesenchymal markers were up-regulated when LLGL1 was knocked-down. Consistent with our microarray analysis, the EMT markers vimentin, KRT17, FBN1, SDC2, L1CAM, and LOXL2 were up-regulated significantly upon inhibition of LLGL1 (Figure 5*A*), and they were partially rescued when OSMR was inhibited (Figure 5*B*). Meanwhile, expression of CSC markers CD44 and CD24 were increased in LLGL1-inhibited Capan2 and SW1990 cells (Figure 5*C* and *D*), and their levels were reduced after knockdown of OSMR (Figure 5*E*). Taken together, we showed that loss of LLGL1 led to the activation of OSMR signaling, which was the major mechanism mediating gemcitabine resistance by inducing cancer stemness and partially activating EMT transition.

Overexpression of LLGL1 Suppressed OSMR Expression and Improved Gemcitabine Response in Gemcitabine-Resistant PANC1 Cells

To show the interaction between LLGL1 and OSMR for the regulation of gemcitabine response, we overexpressed LLGL1 in PANC1 cells, which had a relatively low LLGL1 expression. Overexpression of LLGL1 in PANC1 cells (Figure 6*A*) significantly improved gemcitabine response, which reduced the IC50 of gemcitabine in PANC1 cells approximately 4-fold (IC50 reduced from [parental] 0.3658 ± 0.0520 μmol/L and [Lenti-Ctrl] 0.3877 ± 0.0448 μmol/L to [Lenti-LLGL1] 0.0905 ± 0.0007 μmol/L) (Figure 6*B*). We also observed that up-regulation of LLGL1 significantly decreased OSMR expression (Figure 6*C*) in PANC1 cells and suppressed the luciferase activity of OSMR promoter (Figure 6*D*). LLGL1 plays important roles in establishing cell polarity when forming complexes with discs large protein and Scribble.[25] The Scribble complex was reported to participate in regulating retrovirus-associated DNA sequences/proto-oncogene, serine/threonine kinase/mitogen-activated protein kinase kinase 1/extracellular signal-regulated kinase (ERK) signal transduction cascade.[25,26] We showed that LLGL1 regulated ERK signaling in PDAC. Overexpression of LLGL1 dephosphorylated ERK2 and specificity protein 1 (Sp1) in PANC1 cells (Figure 6*E*). Conversely, knockdown of LLGL1 activated ERK2 in Capan2 and SW1990 cells, which subsequently phosphorylated Sp1 at the Thr453 residue (Figure 6*F*).

LLGL1 Negatively Regulated OSMR Expression by Modulating the Activity of ERK2/Sp1 Signaling

To dissect the mechanism of ERK and Sp1 signaling in regulating OSMR expression, we treated PDAC cells with the ERK inhibitor FR180204 and the Sp1 inhibitor mithramycin A and then studied these effects on OSMR expression. Both treatments effectively reduced the promoter activity of the luciferase reporter containing OSMR promoter (Figure 7*A*) and significantly reduced OSMR expression in LLGL1-inhibited Capan2 and SW1990 cells (Figure 7*B*). To study the role of Sp1 signaling in LLGL1-mediated regulation of OSMR, we first inhibited Sp1 expression by siRNAs and measured the level of OSMR. We showed that knockdown of Sp1 suppressed OSMR expression (Figure 7*C*). Subsequently, we studied the effect of Sp1 depletion on gemcitabine response, and showed that inhibition of Sp1 could reverse gemcitabine resistance in LLGL1-inhibited Capan2 and SW1990 cells (Figure 7*D*). This evidence suggested that ERK2/Sp1 signaling was a major pathway mediating OSMR expression and inducing gemcitabine resistance in LLGL1-inhibited PDAC cells.

A previous study showed that ERK1/ERK2 (p42/p44 mitogen-activated protein kinase) could phosphorylate Sp1 at multiple amino acid sites including Thr453 residue.[27] Phosphorylation of Sp1 at B^{Q}Thr453 mainly enhances its binding activity with DNA and conserved A-T rich sequence (TATA)-binding protein, and prompts the access of transcription

Figure 2. (***See previous page***). **Knockdown of LLGL1 reduced gemcitabine response in Capan2 and SW1990 cells.** (*A*) *Left*: IHC staining for LLGL1 (magnification, 400×) in PDAC tissues and adjacent normal tissues. *Right*: LLGL1 expression was reduced significantly in PDAC tissues compared with adjacent normal tissues (Mann–Whitney *U* test, ***$P < .001$). (*B*) Knockdown of LLGL1 significantly desensitized Capan2 (*left*) and SW1990 cells (*right*) to gemcitabine treatment (2-way analysis of variance, ***$P < .001$). (*C*) LLGL1 regulated the cell proliferation of PDAC cells. Colony formation assay showed that knockdown of LLGL1 induced cell proliferation of Capan2 and SW1990 cells. (*D*) LLGL1 regulated the transforming activity of PDAC cells. Soft agar assay showed that knockdown of LLGL1 induced the transforming activity of Capan2 and SW1990 cells. (*E*) Colony formation assay and soft agar assay showed that overexpression of LLGL1 inhibited the cell proliferation and transforming activity of PANC1 cells. (*F*) *Left*: siRNA interference efficiently reduced LLGL1 expression in Capan2 cells. *Right*: Knockdown of LLGL1 slightly inhibited Rhodamine 123 accumulation in Capan2 cells, and the effect was independent of the presence of 1.0 μmol/L gemcitabine. (*G*) Rhodamine 123 efflux assays, and (*H*) statistical analysis indicated that Rhodamine 123 efflux efficiency was not altered after knockdown of LLGL1 in Capan2 cells (2-way analysis of variance, $P > .05$). *$P < .05$, **$P < .01$, ***$P < .001$, and ****$P < .0001$. Ctrl, control; NC, negative control.

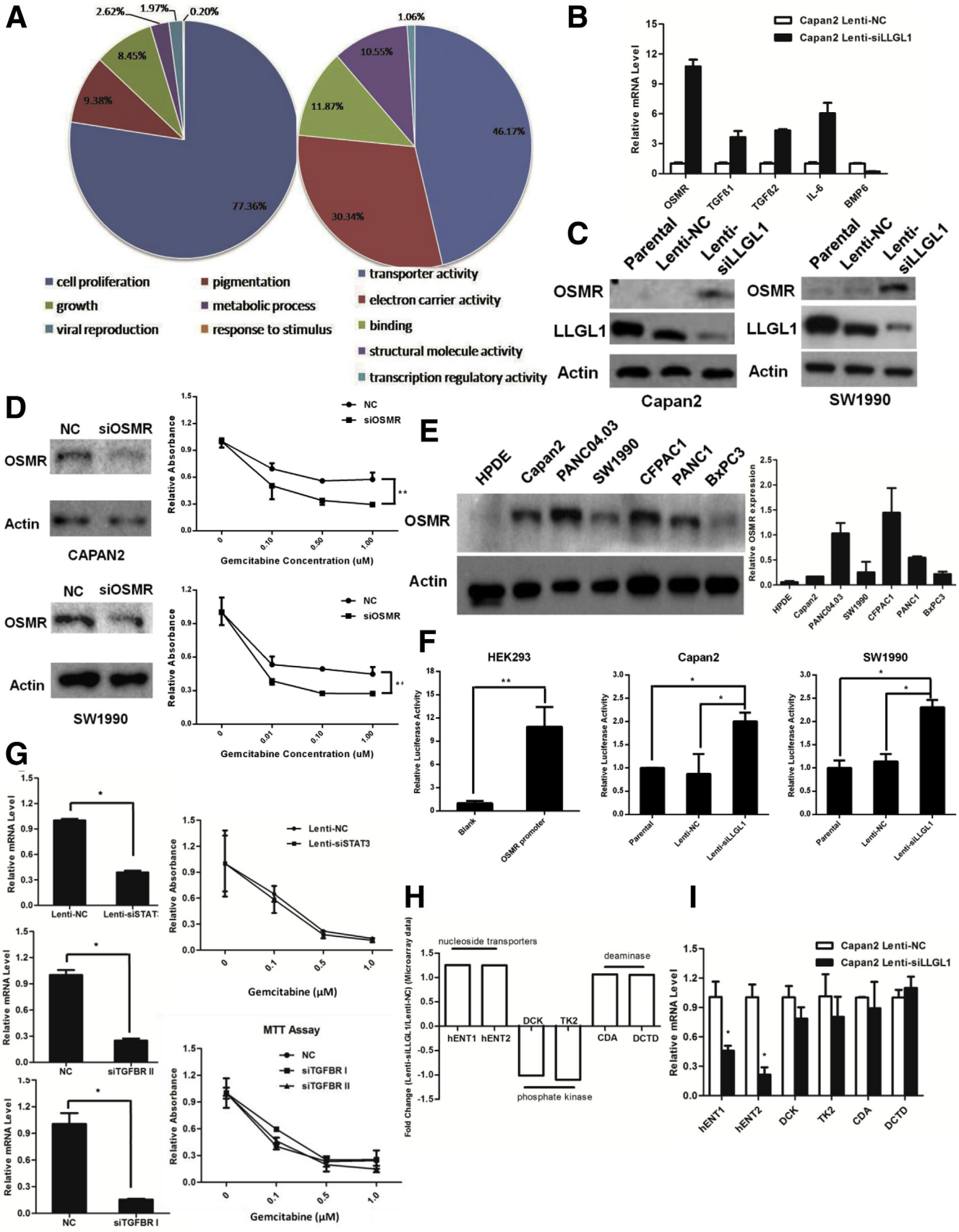
A
2.62%
1.97%
0.20%
8.45%
9.38%
77.36%
1.06%
10.55%
11.87%
46.17%
30.34%
cell proliferation
pigmentation
transporter activity
growth
metabolic process
electron carrier activity
viral reproduction
response to stimulus
binding
structural molecule activity
transcription regulatory activity
B
Capan2 Lenti-NC
Capan2 Lenti-siLLGL1
Relative mRNA Level
OSMR
TGFß1
TGFß2
IL-6
BMP6
C
Parental
Lenti-NC
Lenti-siLLGL1
OSMR
LLGL1
Actin
Capan2
SW1990
D
NC
siOSMR
OSMR
Actin
CAPAN2
SW1990
Relative Absorbance
Gemcitabine Concentration (uM)
E
HPDE
Capan2
PANC04.03
SW1990
CFPAC1
PANC1
BxPC3
Relative OSMR expression
F
HEK293
Capan2
SW1990
Relative Luciferase Activity
Blank
OSMR promoter
Parental
Lenti-NC
Lenti-siLLGL1
G
Relative mRNA Level
Lenti-NC
Lenti-siSTAT3
Relative Absorbance
Gemcitabine (μM)
NC
siTGFBR II
siTGFBR I
MTT Assay
H
nucleoside transporters
deaminase
hENT1
hENT2
DCK
TK2
CDA
DCTD
phosphate kinase
Fold Change (Lenti-siLLGL1/Lenti-NC) (Microarray data)
I
Capan2 Lenti-NC
Capan2 Lenti-siLLGL1

factor IID and other transcriptional-initiating factors to the TATA-less and initiator-less OSMR promoter. We believed that the loss of LLGL1 promoted phosphorylation of Sp1 and facilitated the binding of Sp1 at the OSMR promoter. We then studied the enrichment levels of Sp1 at the OSMR promoter in both gemcitabine-resistant and gemcitabine-sensitive cell lines. By chromatin immunoprecipitation (ChIP), we showed that Sp1 (pThr453) and RNA polymerase II (Pol II) frequently were occupying the OSMR promoter in gemcitabine-resistant PANC1 cells, but not in gemcitabine-sensitive HPDE, Capan2, and SW1990 cells (Figure 7*E*). Knockdown of LLGL1 significantly enriched Sp1 (pThr453) and Pol II at the OSMR promoter in SW1990 cells (Figure 7*F*), whereas ectopic expression of LLGL1 significantly reduced the enrichment of Sp1 (pThr453) and Pol II at the OSMR promoter in PANC1 cells (Figure 7*G*). It showed that LLGL1 inhibited Sp1 binding to the OSMR promoter, which led to the attenuation of gemcitabine resistance in PDAC cells. Taken together, our studies suggest that LLGL1 functioned to repress OSMR expression by activating ERK/Sp1 signaling. Activation of ERK promoted the phosphorylation of Sp1, which led to an increase of binding efficiency at the promoter of OSMR and induced the expression of OSMR.

Discussion

We conducted genome-wide RNAi screening in Capan2 cells and unraveled a novel tumor-suppressive role of LLGL1 in improving gemcitabine response. The tumor-suppressor roles of LLGL1, as well as its cooperators Scribble and Dlg, were reported in Drosophila.[25] Lgl mutation directly could disturb the establishment of basolateral polarity and deregulate various essential signaling pathways including Salvador/Warts/Hippo (SWH), Notch,[28,29] and Wnt in the Drosophila model. Studies have identified frequent losses of LLGL1 in various mammalian tumors including melanoma, glioblastoma, and lung cancer,[13–15] but its role in PDAC largely was unexplored. Our study showed a new tumor-suppressor role of LLGL1 by showing that knockdown of LLGL1 induced gemcitabine resistance in PDAC cells. During gemcitabine treatment, PDAC cells would take up gemcitabine by hENT1 and hENT2. Upon phosphorylation of gemcitabine to its diphosphorylated or triphosphorylated form, gemcitabine induced cell apoptosis in PDAC cells through the inhibition of deoxyribonucleotide synthesis by inactivating the ribonucleotide reductase or direct blockade of DNA elongation during replication. In this study, we illustrated that knockdown of LLGL1 could effectively eliminate the growth-inhibitory effect induced by gemcitabine treatment in Capan2 cells.

We identified OSMR signaling as the downstream target of LLGL1 that mediated gemcitabine resistance. OSMR protein exists as part of the heterodimerized receptor with glycoprotein 130, and activates downstream signaling pathways including Janus kinase/signal transducer and activator of transcription, mitogen-activated protein kinase,[30] and phosphatidylinositol-3-kinase pathways.[31] In addition to its pathogenic role in inflammatory diseases,[32] accumulating studies have pointed to the oncogenic role of OSMR during cancerous development. Up-regulation of OSMR was observed frequently in cancers such as cervical squamous carcinoma and breast cancer.[33,34] A comprehensive analysis of microarray gene expression data from fine-needle aspirates of 278 breast cancer samples showed that OSMR expression was correlated strongly with the level of multiple EMT markers and the level of CSC markers,[33] and also associated significantly with the phosphatidylinositol-3-kinase/protein kinase B signaling pathway.[33] More importantly, the ligand OSM was reported to potently induce EMT and CSC phenotypes in PDAC.[22] Here, we also observed increased expression of mesenchymal markers and CSC markers CD44 and CD24 in PDAC cells after knockdown of LLGL1. Inhibition of OSMR could attenuate the expression of CD24 and CD44, suggesting that OSMR contributed in LLGL1-mediated cancer stemness regulation. However, inhibition of OSMR could only slightly up-regulate mesenchymal markers, indicating that other mechanisms were involved in the regulation of mesenchymal markers in LLGL1-inhibited Capan2 and SW1990 cells. We have uncovered the oncogenic role of OSMR in mediating the gemcitabine resistance of PDAC cells. We postulated that loss of LLGL1 promoted gemcitabine resistance in PDAC cells, which was partially dependent on the activation of OSMR signaling and the subsequent induction of an anti-apoptotic effect and cancer stemness. In addition to OSMR signaling, LLGL1 indirectly may participate in nucleotide transportation regulation, which determined gemcitabine sensitivity in PDAC cells. LLGL1 could regulate hENT1 and hENT2 expression to limit cellular uptake of gemcitabine, which also may contribute to gemcitabine resistance in LLGL1-inhibited PDAC cells. The deficiency of hENT1, a widely abundant and distributed nucleoside transporter in human cells, was validated intriguingly to confer resistance to gemcitabine toxicity by in vitro studies and reduced median survivals from gemcitabine initiation in PDAC patients by

Figure 3. (***See previous page***). **OSMR was the downstream target of LLGL1 mediating gemcitabine resistance.** (*A*) Microarray analysis showed that the expression levels of more than 200 genes were changed by ≥2-fold after knockdown of LLGL1 in Capan2 cells. Gene Ontology analysis showed that most of the candidate genes fell into categories of cell proliferation and transporter activity. (*B*) OSMR, interleukin (IL)6, TGFβ1, and TGFβ2 were up-regulated when LLGL1 was inhibited in Capan2 cells. (*C*) Knockdown of LLGL1 markedly increased OSMR expression in Capan2 and SW1990 cells. (*D*) Knockdown of OSMR by siRNAs reversed gemcitabine resistance in LLGL1-inhibited Capan2 and SW1990 cells. (*E*) Profiling of OSMR expression levels in HPDE and PDAC cells showed that OSMR was more highly expressed in PDAC cells than in HPDE cells. (*F*) Transfection of reporter containing OSMR promoter into HEK293 cells showed an increase in luciferase activity compared with blank vectors. Knockdown of LLGL1 enhanced the promoter activity of OSMR in capan2 and SW1990 cells (2-way analysis of variance, $^{**}P < .01$). (*G*) Knockdown of signal transducer and activator of transcription 3 (STAT3), TGFBRI, and TGFBRII had no effect on gemcitabine response in Capan2-siLLGL1 cells. Janus kinase/STAT3 signaling and TGFβ signaling were not involved in LLGL1-associated gemcitabine resistance. $^{*}P < .05$, $^{**}P < .01$. CDA, cytidine deaminase; DCK, deoxycytidine kinase; DCTD, dCMP deaminase; mRNA, messenger RNA; NC, negative control; TGFBR, transforming growth factor beta receptor.

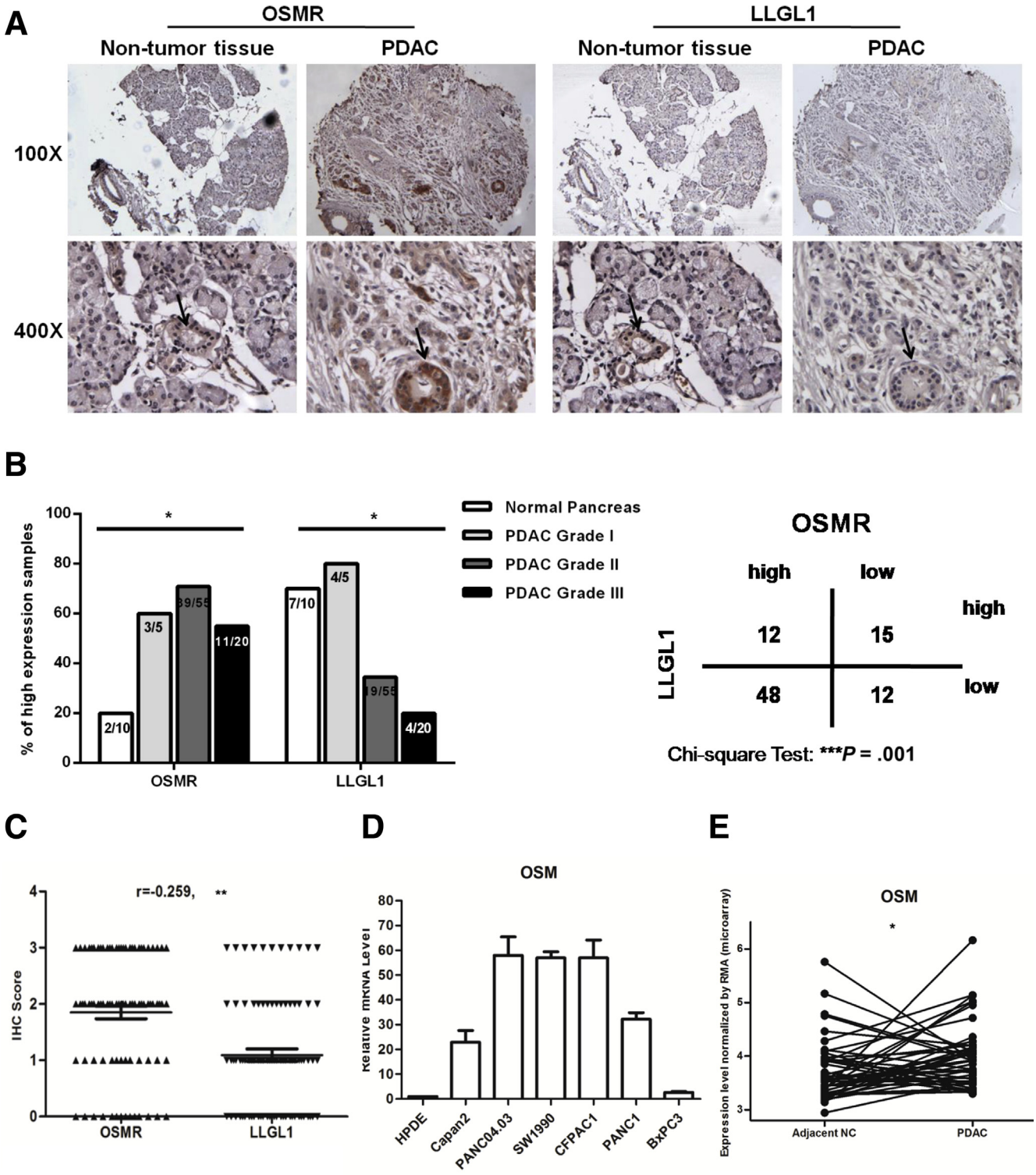

Figure 4. OSMR expression was correlated negatively with LLGL1 expression in human PDAC tissues. (*A*) IHC staining of OSMR and LLGL1 were performed in the human PDAC tissue microarray. (*B*) *Left*: Scoring of the staining intensity showed that the OSMR expression level was higher in all stages of PDAC tissues compared with that in nontumor tissues (Kruskal–Wallis H test, $^{*}P < .05$). Meanwhile, the level of LLGL1 was higher in nontumor and low-grade PDAC (grade I) compared with high-grade PDAC (grades II and III) (Kruskal–Wallis H test, $^{*}P < .05$). *Right*: The IHC staining score was subdivided into 2 categories. IHC scores of 0 and 1 were grouped into low expression, and IHC scores of 2 and 3 were grouped into high expression. The chi-square test showed that the expression of LLGL1 was associated with that of OSMR ($^{***}P = .001$). (*C*) Pearson correlation analysis showed that expression of OSMR was correlated negatively with LLGL1 expression in PDAC specimens ($R^2 = -0.259$, $^{**}P < .01$). (*D*) OSM expression was increased significantly in K-Ras mutant Capan2, PANC04.03, SW1990, CFPAC1, and PANC1 cells, but not in HPDE cells and K-Ras wild-type BxPC3 cells. (*E*) Compared with adjacent nontumor tissues (adjacent NC), PDAC tissues showed a higher expression level of OSM in a German cohort of 45 paired specimens obtained from a public database (paired *t* test, $^{*}P < .05$). $^{*}P < .05$, $^{**}P < .01$, $^{***}P < .001$.

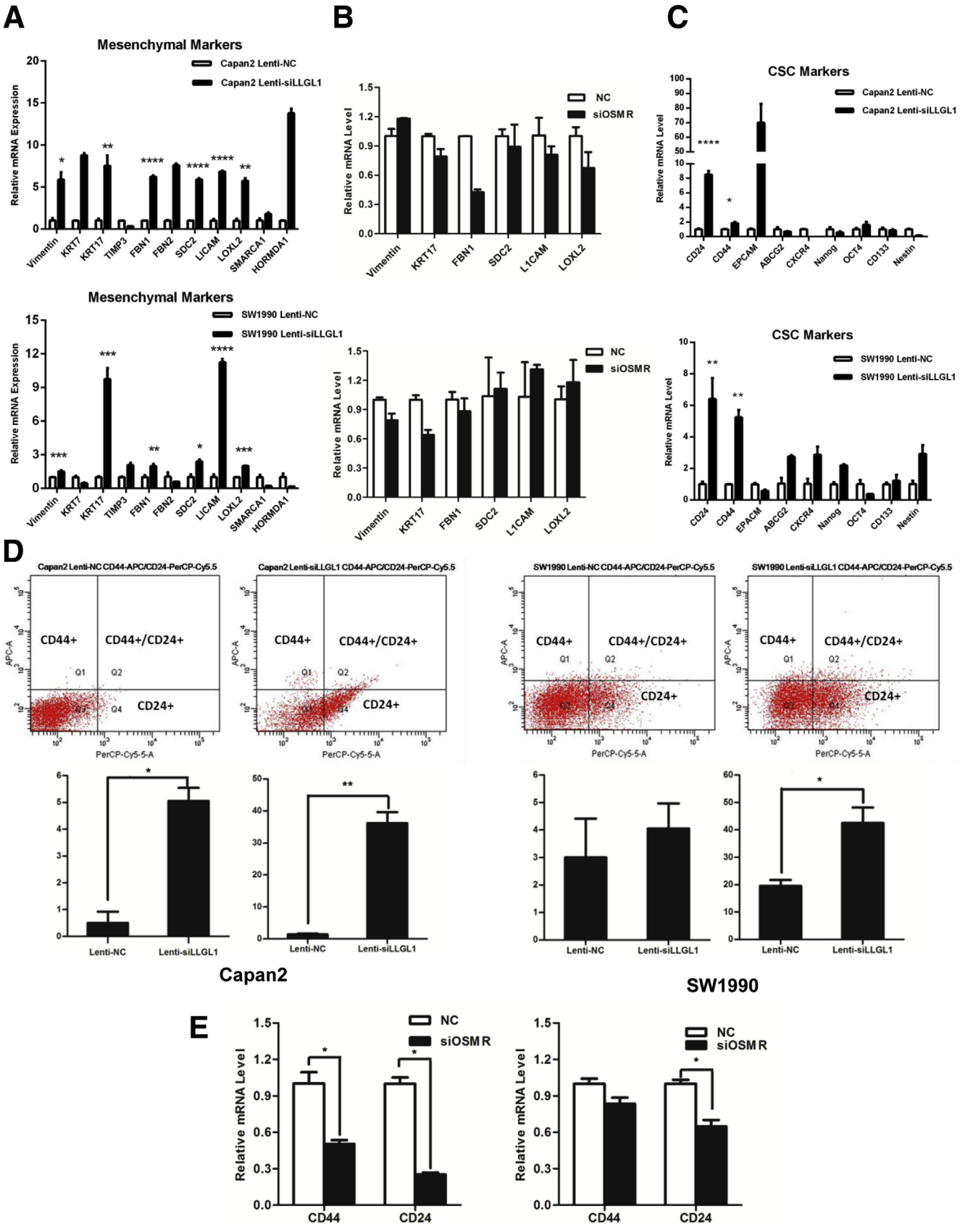
A
Mesenchymal Markers
Capan2 Lenti-NC
Capan2 Lenti-siLLGL1
Relative mRNA Expression
Vimentin
KRT7
KRT17
TIMP3
FBN1
FBN2
SDC2
LICAM
LOXL2
SMARCA1
HORMDA1
B
NC
siOSMR
Relative mRNA Level
Vimentin
KRT17
FBN1
SDC2
L1CAM
LOXL2
C
CSC Markers
Capan2 Lenti-NC
Capan2 Lenti-siLLGL1
Relative mRNA Level
CD24
CD44
EPACM
ABCG2
CXCR4
Nanog
OCT4
CD133
Nestin
Mesenchymal Markers
SW1990 Lenti-NC
SW1990 Lenti-siLLGL1
Relative mRNA Expression
NC
siOSMR
Relative mRNA Level
CSC Markers
SW1990 Lenti-NC
SW1990 Lenti-siLLGL1
Relative mRNA Level
D
Capan2 Lenti-NC CD44-APC/CD24-PerCP-Cy5.5
Capan2 Lenti-siLLGL1 CD44-APC/CD24-PerCP-Cy5.5
SW1990 Lenti-NC CD44-APC/CD24-PerCP-Cy5.5
SW1990 Lenti-siLLGL1 CD44-APC/CD24-PerCP-Cy5.5
CD44+
CD44+/CD24+
CD24+
APC-A
PerCP-Cy5-5-A
Lenti-NC
Lenti-siLLGL1
Capan2
SW1990
E
NC
siOSMR
Relative mRNA Level
CD44
CD24

immunohistochemistry.[35] hENT1 has been proven to be a potential predictive biomarker of improved survival in PDAC patients treated with gemcitabine.[36] It has been shown that simultaneous preservation of hENT1 and deoxycytidine kinase in PDAC tumors predicted longer survival times in patients treated with adjuvant gemcitabine therapy.[37] The underlying mechanisms on the regulation of hENT1 and hENT2 by LLGL1 are worthy of further investigation.

Studies have shown that loss of Lgl resulted in increased expression of cell-cycle cyclin E and death-associated inhibitor of apoptosis 1, in which both are targets of warts in Drosophila ovary cells.[28] The reports suggested that the repression of warts signaling was pivotal to promote EMT transition, cell proliferation, and motility.[28,38,39] We believe that other pathways regulated by LLGL1 such as ERK/Sp1 signaling or SWH signaling could be the alternative mechanisms that regulated EMT. The promoters of all up-regulated mesenchymal markers contained multiple Sp1 binding sites. SWH signaling regulated gene expression by the binding of its effectors YES-associated protein and PDZ-binding Motif to other transcriptional factors such as TEA domain family members. The role of SWH signaling in LLGL1 regulation needs further investigation.

A recent study showed that activation of ERK signaling during gemcitabine treatment resulted in the generation of gemcitabine resistance.[40] Phosphorylation of Sp1 at Thr453 of domain B^Q could physically intensify and stabilize direct interaction of the TATA-less promoter and the TATA-binding protein accessory factor transcription factor IID,[27] and subsequently initiate TATA-less gene transcription.[41] Consistent with this observation, OSMR has a TATA-less, initiator-less, but Sp1-binding-site–rich promoter. Knockdown of LLGL1 significantly increased the accumulation of Sp1 (pThr453) and Pol II at the OSMR promoter, while up-regulation of LLGL1 decreased the accumulation of Sp1 (pThr453) and Pol II at the OSMR promoter. We concluded that LLGL1 expression negatively regulated ERK2/Sp1 signaling and subsequently modulated OSMR expression. As a cytoplasm-localized protein, the molecular mechanism underlying LLGL1-mediated up-regulation of OSMR still is unexplored. Studies already have shown that Scribble complex and Par complex antagonized each other through the dynamic phosphorylation and translocalization of LLGL1 between the apical and basolateral membrane.[42] We hypothesized that knockdown of LLGL1 allowed the release of phosphorylation sites in an atypical protein kinase C/human homologue of partitioning defective protein 6 complex, which then phosphorylated its substrate of ERK2 in PDAC cells. Future studies are warranted to prove this hypothesis.

In conclusion, our study potentiated the development of the novel biomarker LLGL1 in predicting gemcitabine response in patients with PDAC, because loss of LLGL1 expression is associated with low sensitivity to gemcitabine. We provided the molecular basis for the development of adjuvant therapy based on LLGL1 expression because we showed that overexpression of LLGL1 could elicit a satisfactory gemcitabine response in PDAC cells. The LLGL1-regulated regulatory axis of ERK2/Sp1-OSMR also provides numerous targets that allow the development of novel therapeutic strategies against gemcitabine resistance.

Materials and Methods

Cell Lines and Drug Treatment

BxPC3, Capan2, CFPAC1, PANC1, PANC04.03, SW1990, HEK293, and HEK293T cells were obtained from American Type Culture Collection (Manassas, VA). The HPDE cell line was a gift from Dr Ming-Sound Tsao (University Health Network, Ontario Cancer Institute and Princess Margaret Hospital Site, Toronto, Canada) and was maintained according to the publication.[43] For drug treatments, designated dosages of gemcitabine (Lilly France S.A.S., Neuilly-sur-Seine, Lilly France SASU), 100 μmol/L of FR180204, and 500 nmol/L of mithramycin A (Tocris Bioscience, Minneapolis, MN) were added to cultured cells and incubated for 48–72 hours.

Clinical Specimens and Tissue Microarray

Sixty pairs of PDAC specimens and adjacent normal tissues were collected from patients who underwent surgical resection at the Prince of Wales Hospital. For the comparison of disease-free survival between patients with and without LLGL1 expression, 29 patients with surgical resection tumors were collected from the Sun Yat-sen Memorial Hospital, Sun Yat-sen University (Guangzhou, China). The inclusion criteria were as follows: a primary diagnosed PDAC and gemcitabine was the single agent in adjuvant chemotherapy; the exclusion criteria were as follows: chemotherapy of fewer than 6 cycles and stage IV disease. Disease-free survival was taken as the main end point. The study was performed with the approval of the Chinese University of Hong Kong Clinical Research Ethical Committee and the Sun Yat-sen Memorial Hospital Ethical Committee, and informed consent was obtained from all patients recruited. Tissue microarray slides, containing 87 PDAC cases and 10 normal cases, were purchased from US Biomax (PA2082; Rockville, MD).

Figure 5. (*See previous page*). **LLGL1 regulated the expression of mesenchymal and gemcitabine-resistance associated CSC markers in PDAC cells.** (*A*) Knockdown of LLGL1 increased the expression of several mesenchymal markers including vimentin, KRT17, FBN1, SDC2, L1CAM, and LOXL2 in Capan2 and SW1990 cells. (*B*) Knockdown of OSMR could partially reverse the up-regulation of mesenchymal markers in LLGL1-inhibited Capan2 cells (*upper panel*) and SW1990 cells (*lower panel*). (*C*) The levels of several gemcitabine-resistance associated CSC markers were measured by qRT-PCR in LLGL1-inhibited Capan2 and SW1990 cells. It showed that both CD44 and CD24 were up-regulated after knockdown of LLGL1. (*D*) Flow cytometric analysis of cell surface expression of CD44 and CD24 indicated that both were increased after the inhibition of LLGL1 in Capan2 (*left panel*) and SW1990 cells (*right panel*). (*E*) Knockdown of OSMR significantly reduced the expression of CD44 and CD24 in LLGL1-inhibited Capan2 (*left panel*) and SW1990 cells (*right panel*). $^*P < .05$, $^{**}P < .01$, $^{***}P < .001$, and $^{****}P < .0001$. mRNA, messenger RNA; NC, negative control; PerCP, Peridinin-Chlorophyll-Protein.

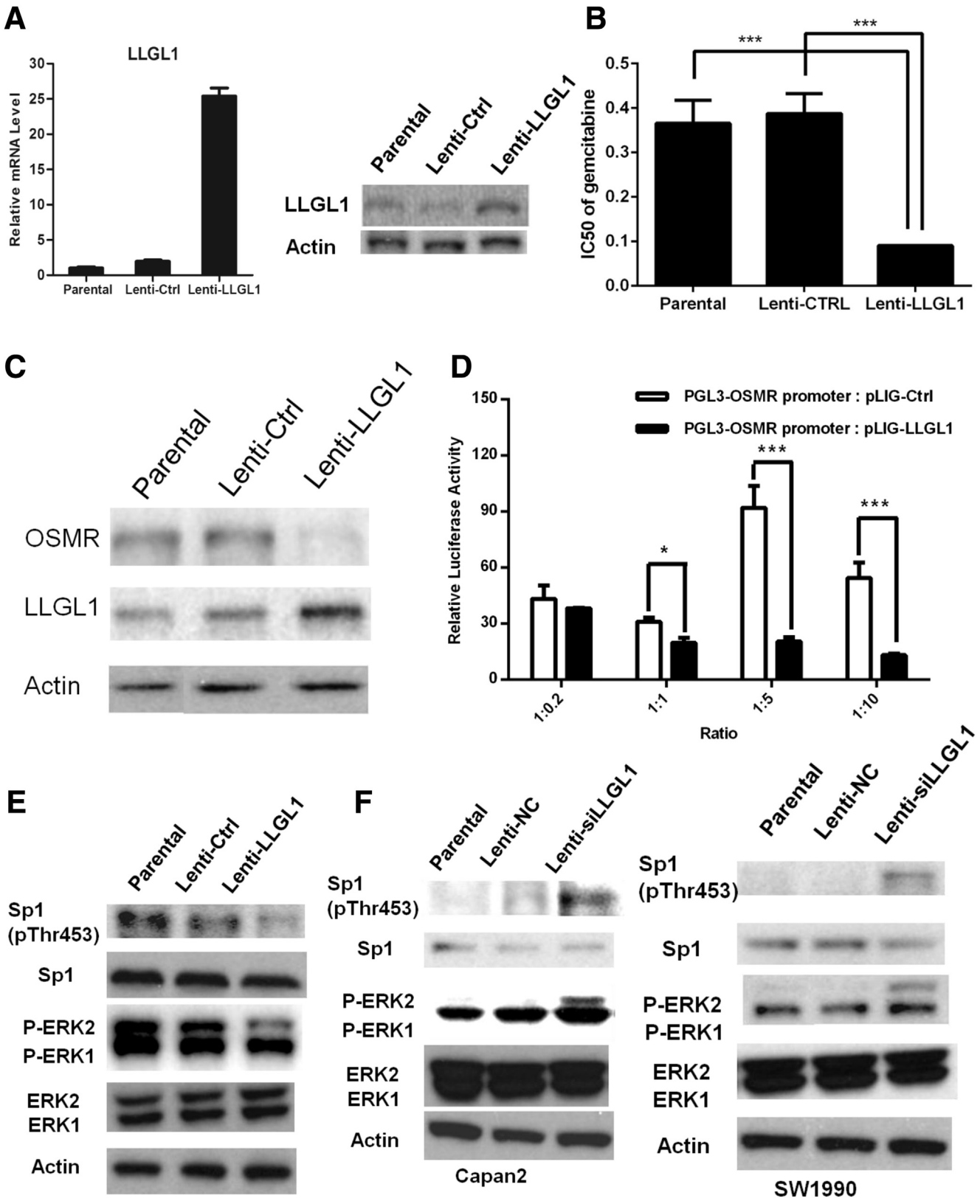

Figure 6. LLGL1 inactivated ERK2/Sp1 signaling to suppress OSMR expression. (*A*) Increased LLGL1 expression was observed in PANC1 cells after transduction with lenti-LLGL1. (*B*) LLGL1 overexpression sensitized PANC1 cells to gemcitabine treatment (2-way analysis of variance, ***$P < .001$), and (*C*) Western blot showed that overexpression of LLGL1 inhibited OSMR expression. (*D*) Co-transfection of reporter containing OSMR promoter with pLIG-LLGL1 was performed. It showed that overexpression of LLGL1 significantly reduced the promoter activity of OSMR. (*E*) Overexpression of LLGL1 reduced the phosphorylation of ERK2 and Sp1 in PANC1 cells, while (*F*) knockdown of LLGL1 increased ERK2 and Sp1 phosphorylation in Capan2 and SW1990 cells. *$P < .05$, ***$P < .001$. Ctrl, control; mRNA, messenger RNA; P-ERK, phosphorylated extracellular signal-regulated kinase.

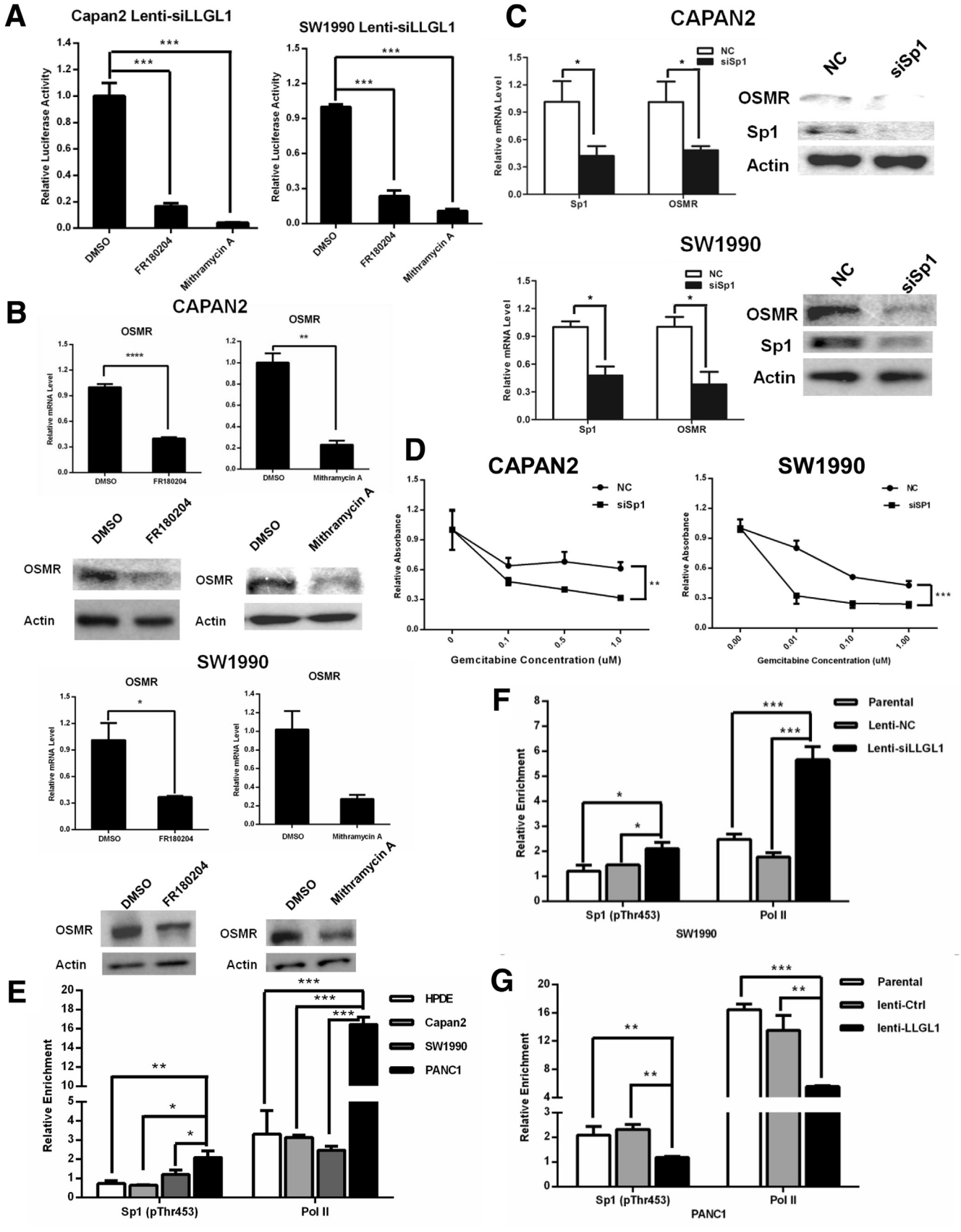
A
Capan2 Lenti-siLLGL1
SW1990 Lenti-siLLGL1
Relative Luciferase Activity
DMSO
FR180204
Mithramycin A
B
CAPAN2
OSMR
Relative mRNA Level
Actin
SW1990
C
CAPAN2
NC
siSp1
Sp1
OSMR
SW1990
D
CAPAN2
SW1990
Relative Absorbance
Gemcitabine Concentration (uM)
E
HPDE
Capan2
SW1990
PANC1
Relative Enrichment
Sp1 (pThr453)
Pol II
F
Parental
Lenti-NC
Lenti-siLLGL1
SW1990
G
Parental
lenti-Ctrl
lenti-LLGL1
PANC1

Genome-Wide RNAi Screening

GeneNet lentiviral siRNA libraries (50K) was purchased from System Biosciences (Mountain View, CA), and transduced into gemcitabine-sensitive Capan2 cells (2×10^6)[18] according to the manufacturer's protocol, with an expected multiplicity of infection of 1 (average of 1 copy of integrated siRNA construct per cell). Transduced cells then were divided into 2 groups: control group and treatment group. Cells in the treatment group were treated with 2 μmol/L gemcitabine for 6 days for resistant clone selection, whereas no drug was added to the control group in which such drug treatment could cause complete cell death in parental Capan2 cells. In turn, RNA was extracted from the selected gemcitabine-resistant clones and the control group for biotinylated siRNA effector amplification. Finally, the biotin-labeled amplified siRNA targets were quantified using the Affymetrix GeneChip Human Genome U133 plus 2.0 Array (Affymetrix, Santa Clara, CA). Data then were analyzed by Partek software (St. Louis, MO).

Drug Cytotoxicity Assay, Colony Formation Assay, and Soft Agar Assay

The cytotoxicity of gemcitabine in PDAC cells was assessed with a 3-(4,5-dimethylthiazol-2-yl)-2,5-diphenyltetrazolium bromide (MTT) assay (USB Corporation, Cleveland, OH). PDAC cells (5×10^3 per well) were seeded in a 96-well plate for gemcitabine treatment. The working MTT solution was added to the cultured 96-well plates. After 2–4 hours of incubation at 37°C in darkness, MTT solution was removed and 100 uL dimethyl sulfoxide was added to the plates. The absorbance was measured at λ570 nm. The relative absorbance was calculated by optical $\text{density}_{\text{treatment}}/\text{optical density}_{\text{control}}$. All drug cytotoxicity assays were repeated 3 times. For siRNA gemcitabine cotreatment, PDAC cells first were transfected with siRNAs for 72 hours before they were treated with gemcitabine.

For the colony formation assay, 5×10^2 cells were seeded in 6-well plates and incubated at 37°C for 2–3 weeks. After that, the cells were stained with Coomassie blue. For the soft agar assay, 5×10^3 cells were plated in 0.35% agar over a layer of 0.5% agar containing complete Dulbecco's modified Eagle medium in a 6-well plate. Cells were incubated at 37°C for 2–3 weeks, and then stained with 0.005% crystal violet. The number of colonies was counted under light microscopy. The assays were repeated 3 times.

Plasmid, Lentivirus Production, and Infection

iLenti-GFP LLGL1 siRNAs were obtained from Applied Biological Materials, Inc (Richmond, BC). Full-length human LLGL1 cDNA was cloned into our established lentiviral vector (pLIG) that could co-express green fluorescent protein.[44] The Lenti–small interfering LLGL1 (siLLGL1) and Lenti-LLGL1 then were packaged by co-transfecting the transfer plasmids and the packaging plasmids: pMDLg/pRRE, pRSV-REV, and pCMV-VSVG into HEK293T cells.[45] Cancer cells (5×10^4) were seeded in 24-well plates overnight before being transduced with lentivirus in the presence of 8 μg/mL hexadimethrine bromide (Sigma, St Louis, MO).

Gene Expression Microarray analysis

Gene expression microarray analyses were conducted with GeneChip Human Genome U133 plus 2.0 Array ChIP (Affymetrix) as described previously.[46] Total RNA from Capan2 Lenti-NC and Capan2 Lenti-siLLGL1 cells were subjected to quality checking. Raw data were accessible on Gene Expression Omnibus. Data then were analyzed with Partek software. All the candidate genes selected for Gene Ontology enrichment analysis were at least 2-fold differentially expressed. Public gene expression data for a German cohort of 45 paired PDAC samples and adjacent nontumor tissues were acquired from the National Center for Biotechnology Information's Gene Expression Omnibus database.[47]

siRNA transfection. siRNAs targeting LLGL1, OSMR, Sp1, Dlg1, Scribble, ring finger protein 126, glutamate ionotropic receptor kainate type subunit 2, erythropoietin receptor, and interleukin 6 (Shanghai GenePharma Co, Ltd, Shanghai, China) were transfected into cells using the DharmaFECT 1 siRNA transfection reagent (Thermo Scientific, Lafayette, CO), according to the manufacturer's protocol.

Total RNA extraction and qRT-PCR. Total RNA was extracted from cultured cells using the TRIzol total RNA isolation reagent (Invitrogen, Waltham, MA), according to the manufacturer's instructions. cDNA then was synthesized using the High-Capacity cDNA Reverse Transcription Kit (Applied Biosystems, Waltham, MA). To determine the expression levels of target genes, gene primers were obtained from PrimerBank (http://pga.mgh.harvard.edu) and qRT-PCR was performed using SYBR Green PCR Master Mix (Takara Bio, Inc, Shiga, Japan) with the ABI 7900HT Fast Real-Time PCR detection system. The relative amount of expression was measured by comparative CT ($2^{-\text{delta delta comparative CT}}$), which was normalized with the endogenous reference control gene glyceraldehyde-3-phosphate dehydrogenase.

Protein extraction and Western blot analysis. Total protein was extracted from cultured cells using RIPA lysis buffer supplemented with protease inhibitors. Standard Western blot was performed to determine the expression

Figure 7. (***See previous page***). **Activation of ERK2/Sp1 signaling and recruitment of Sp1(pThr453) to the OSMR promoter induced up-regulation of OSMR.** (*A*) FR180204 (100 μmol/L) and mithramycin A (500 nmol/L) treatment effectively reduced the OSMR promoter activity in Capan2 and SW1990 cells, and (*B*) inhibited OSMR expression in LLGL1-inhibited Capan2 and SW1990 cells. (*C*) Knockdown of Sp1 by siRNAs suppressed OSMR expression and (*D*) improved gemcitabine response in LLGL1-inhibited Capan2 and SW1990 cells (2-way analysis of variance, $^{**}P < .01$). (*E*) Sp1(pThr453) and Pol II were enriched at the OSMR promoter in gemcitabine-resistant PANC1 cells compared with HPDE cells, as well as gemcitabine-sensitive Capan2 and SW1990 cells. (*F*) Increased enrichments of Sp1(pThr453) and Pol II were observed at the OSMR promoter in SW1990 cells upon knockdown of LLGL1. (*G*) Overexpression of LLGL1 reduced enrichment of Sp1 (pThr453) and Pol II in PANC1 cells. $^{*}P < .05$, $^{**}P < .01$, $^{***}P < .001$, and $^{****}P < .0001$. DMSO, dimethyl sulfoxide; mRNA, messenger RNA; NC, negative control.

levels of target proteins. Protein samples were separated by sodium dodecyl sulfate–polyacrylamide gel electrophoresis and blotted onto a polyvinylidene difluoride membrane (Bio-Rad, Hercules, CA). The membrane then was blocked and probed at 4°C overnight with anti-actin, anti-ERK1/2, anti–phospho-ERK1/2, anti-Sp1 (Cell Signaling Technology, Danvers, MA), anti-Sp1 (pThr453) (Abcam, Inc, Cambridge, MA), anti-LLGL1 (Novus Biologicals, Littleton, CO), or anti-OSMR (Santa Cruz Biotechnology, Santa Cruz, CA) diluted with 5% nonfat dry milk (Santa Cruz Biotechnology) in Tris-buffered saline with Tween 20, followed by the respective secondary peroxidase-conjugated antibody incubation, and chemiluminescence signal was developed by ECL Plus Western Blot Detection Reagents (GE Healthcare Life Sciences, Piscataway, NJ).

ChIP. ChIP was performed using the SimpleChIP Enzymatic Chromatin IP Kit Magnetic Beads (Cell Signaling Technology). Cross-linked chromatin was incubated with anti-H3 (positive control), anti-IgG (negative control; Cell Signaling Technology), anti-Sp1 (pThr453) (ab59257; Abcam), and anti–Pol II (2019508; Millipore, Billerica, MA) overnight at 4°C with rotation. The precipitated DNA was quantitated by qPCR and normalized by respective 2% input.

Rhodamine-123 accumulation and efflux assay. Capan2 cells transfected with either negative control of small interfering RNA or siLLGL1 were incubated with or without gemcitabine 1.0 umol/L for 48 hours and then were resuspended in medium (1×10^6/mL). Subsequently, 10 μg/mL Rhodamine 123 was added and the cells were cultured in an incubator with 37°C 5% CO_2 for 30 minutes, and then washed with medium twice. After resuspension in medium, they were incubated in the incubator for 0, 30, 60, and 120 minutes, followed by washing with ice-cold phosphate-buffered saline twice. Rhodamine-123 then was detected by flow cytometry (BD Bioscience, Franklin Lakes, NJ) at 488/530 nm.

Fluorescence-activated cell sorting. Cells (up to 1×10^6) were trypsinized, washed with fluorescence-activated cell sorter buffer (1× phosphate-buffered saline, 2% fetal bovine serum), and then blocked with blocking buffer (1× phosphate-buffered saline, 10% normal human serum). The cells were incubated with Allophycocyanin mouse anti-CD44 and Peridinin-Chlorophyll-Protein–Cy 5.5 mouse anti-CD24 (BD Bioscience) for 30–45 minutes at 4°C. Isotype-matched mouse immunoglobulins (BD Bioscience) served as controls. Flow cytometry was conducted using BD LSRFortessa (BD Bioscience, Franklin Lakes, NJ). Data were analyzed by BD FACSDiva software.

Statistical Analysis

GraphPad Prism 5 (GraphPad Software, La Jolla, CA) and SPSS 16.0 statistical software (SPSS, Inc, Chicago, IL) were used for statistical analysis. Statistical tests for data analysis included a 2-tailed Student *t* test, paired *t* test, Fisher exact test, Pearson correlation coefficient, Kruskal–Wallis H test, Mann–Whitney *U* test, 2-way analysis of variance test, and the Gehan–Breslow–Wilcoxon test for survival curve comparison. Data were presented as means ± SD. *P* values less than .05 were considered statistically significant.

Ethics Approval and Consent to Participate

Surgical resected tumors from 29 patients were collected from the Sun Yat-sen Memorial Hospital, Sun Yat-sen University (Guangzhou, China). The study was performed with approval of the Chinese University of Hong Kong Clinical Research Ethical Committee and the Sun Yat-sen Memorial Hospital Ethical Committee, and informed consent was obtained from all patients recruited. Animal handling and experimental procedures were approved by the Animal Experimental Ethics Committee of the institute.

References

1. Siegel RL, Mille KD, Jemal A. Cancer statistics, 2020 CA Cancer. J Clin 2020;70:7–30.
2. Yeo CJ, Cameron JL, Sohn TA, Lillemoe KD, Pit HA, Talamini MA, Hruban RH, Ord SE, Sauter PK, Coleman J, Zahurak ML, Grochow LB, Abrams RA. Six hundred fifty consecutive pancreaticoduodenectomies in the 1990s: pathology, complications, and outcomes. Ann Surg 1997;226:248–257.
3. Ducreux M, Boige V, Malka D. Treatment of advanced pancreatic cancer. Semin Oncol 2007;34:S25–S30.
4. Hong SP, Wen J, Bang S, Park S, Song SY. CD44-positive cells are responsible for gemcitabine resistance in pancreatic cancer cells. Int J Cancer 2009; 125:2323–2331.
5. Mahon PC, Baril P, Bhakta V, Chelala C, Caulee K, Harada T, Lemoine NR. S100A4 contributes to the suppression of BNIP3 expression, chemoresistance, and inhibition of apoptosis in pancreatic cancer. Cancer Res 2007;67:6786–6795.
6. Arumugam T, Simeone DM, Van Golen K, Logsdon CD. S100P promotes pancreatic cancer growth, survival, and invasion. Clin Cancer Res 2005;11:5356–5364.
7. Eibl G, Takata Y, Boros LG, Liu J, Okada Y, Reber HA, Hines OJ. Growth stimulation of COX-2-negative pancreatic cancer by a selective COX-2 inhibitor. Cancer Res 2005;65:982–990.
8. Arumugam T, Ramachandran V, Fournier KF, Wang H, Marquis L, Abbruzzese JL, Gallick GE, Logsdon CD, McConkey DJ, Choi W. Epithelial to mesenchymal transition contributes to drug resistance in pancreatic cancer. Cancer Res 2009;69:5820–5828.
9. Betschinger J, Mechtler K, Knoblich JA. The Par complex directs asymmetric cell division by phosphorylating the cytoskeletal protein Lgl. Nature 2003;422:326–330.
10. Dollar GL, Weber U, Mlodzik M, Sokol SY. Regulation of lethal giant larvae by dishevelled. Nature 2005; 437:1376–1380.
11. Sripathy S, Lee M, Vasioukhin V. Mammalian Llgl2 is necessary for proper branching morphogenesis during placental development. Mol Cell Biol 2011; 31:2920–2933.
12. Vasioukhin V. Lethal giant puzzle of Lgl. Dev Neurosci 2006;28:13–24.
13. Kuphal S, Wallner S, Schimanski CC, Bataille F, Hofer P, Strand S, Strand D, Bosserhoff AK. Expression of Hugl-1 is strongly reduced in malignant melanoma. Oncogene 2006;25:103–110.

14. Gont A, Hanson JE, Lavictoire SJ, Parolin DA, Daneshmand M, Restall IJ, Soucie M, Nicholas G, Woulfe J, Kassam A, Da Silva VF, Lorimer IA. PTEN loss represses glioblastoma tumor initiating cell differentiation via inactivation of Lgl1. Oncotarget 2013;4:1266–1279.
15. Yang W, Zhou C, Luo M, Shi X, Li Y, Sun Z, Zhou F, Chen Z, He J. MiR-652-3p is upregulated in non-small cell lung cancer and promotes proliferation and metastasis by directly targeting Lgl1. Oncotarget 2016; 7:16703–16715.
16. Biesterfeld S, Kauhausen A, Kost C, Gockel I, Schimanski CC, Galle PR. Preservation of HUGL-1 expression as a favourable prognostic factor in pancreatic carcinoma. Anticancer Res 2012;32:3153–3159.
17. Song J, Peng XL, Ji MY, Ai MH, Zhang JX, Dong WG. Hugl-1 induces apoptosis in esophageal carcinoma cells both in vitro and in vivo. World J Gastroenterol 2013; 19:4127–4136.
18. Giroux V, Malicet C, Barthet M, Gironella M, Archange C, Dagorn JC, Vasseur S, Iovanna JL. p8 is a new target of gemcitabine in pancreatic cancer cells. Clin Cancer Res 2006;12:235–241.
19. Qin Y, Deng WG, Ekmekcioglu S, Grimm EA. Identification of unique sensitizing targets for anti-inflammatory CDDO-Me in metastatic melanoma by a large-scale synthetic lethal RNAi screening. Pigment Cell Melanoma Res 2013;26:97–112.
20. Nishiyama-Fujita Y, Shimizu T, Sagawa M, Uchida H, Kizak M. The role of TC-PTP (PTPN2) in modulating sensitivity to imatinib and interferon-alpha in CML cell line, KT-1 cells. Leuk Res 2013;37:1150–1155.
21. Twentyman PR, Rhodes T, Rayner S. A comparison of rhodamine 123 accumulation and efflux in cells with P-glycoprotein-mediated and MRP-associated multidrug resistance phenotypes. Eur J Cancer 1994; 30A:1360–1369.
22. Young JD, Yao SY, Sun L, Cass CE, Baldwin SA. Human equilibrative nucleoside transporter (ENT) family of nucleoside and nucleobase transporter proteins. Xenobiotica 2008;38:995–1021.
23. Mackey JR, Mani RS, Selner M, Mowles D, Young JD, Belt JA, Crawford CR, Cass CE. Functional nucleoside transporters are required for gemcitabine influx and manifestation of toxicity in cancer cell lines. Cancer Res 1998;58:4349–4357.
24. Smigiel JM, Parameswaran N, Jackson MW. Potent EMT and CSC phenotypes are induced by oncostatin-M in pancreatic cancer. Mol Cancer Res 2017; 15:478–488.
25. Humbert PO, Grzeschik NA, Brumby AM, Galea R, Elsum I, Richardson HE. 2008 Control of tumourigenesis by the Scribble/Dlg/Lgl polarity module. Oncogene 2017; 27:6888–6907.
26. Massimi P, Narayan N, Thomas M, Gammoh N, Strand S, Strand D, Banks L. Regulation of the hDlg/hScrib/Hugl-1 tumour suppressor complex. Exp Cell Res 2008; 314:3306–3317.
27. Milanini-Mongiat J, Pouysségur J, Pagès G. Identification of two Sp1 phosphorylation sites for p42/p44 mitogen-activated protein kinases: their implication in vascular endothelial growth factor gene transcription. J Biol Chem 2002;277:20631–20639.
28. Zhao M, Szafranski P, Hall CA, Goode S. Basolateral junctions utilize warts signaling to control epithelial-mesenchymal transition and proliferation crucial for migration and invasion of drosophila ovarian epithelial cells. Genetics 2008;178:1947–1971.
29. Langevin J, Le Borgne R, Rosenfeld F, Gho M, Schweisguth F, Bellaïche Y. Lethal giant larvae controls the localization of notch-signaling regulators numb, neuralized, and Sanpodo in Drosophila sensory-organ precursor cells. Curr Biol 2005;15:955–962.
30. Tiffen PG, Omidvar N, Marquez-Almuina N, Croston D, Watson CJ, Clarkson RW. A dual role for oncostatin M signaling in the differentiation and death of mammary epithelial cells in vivo. Mol Endocrinol 2008; 22:2677–2688.
31. Drechsler J, Grotzinger J, Hermanns HM. Characterization of the rat oncostatin M receptor complex which resembles the human, but differs from the murine cytokine receptor. PLoS One 2012;7:e43155.
32. Lin YZ, Li RN, Lin CH, Ou TT, Wu CC, Tsai WC, Liu HW, Yen JH. Association of OSMR gene polymorphisms with rheumatoid arthritis and systemic lupus erythematosus patients. Autoimmunity 2014;47:23–26.
33. West NR, Murphy LC, Watson PH. Oncostatin M suppresses oestrogen receptor-alpha expression and is associated with poor outcome in human breast cancer. Endocr Relat Cancer 2012;19:181–195.
34. Winder DM, Chattopadhyay A, Muralidhar B, Bauer J, English WR, Zhang X, Karagavriilidou K, Roberts I, Pett MR, Murphy G, Coleman N. Overexpression of the oncostatin M receptor in cervical squamous cell carcinoma cells is associated with a pro-angiogenic phenotype and increased cell motility and invasiveness. J Pathol 2011;225:448–462.
35. Spratlin J, Sangha R, Glubrecht D, Dabbagh L, Young JD, Dumontet C, Cass C, Lai R, Mackey JR. The absence of human equilibrative nucleoside transporter 1 is associated with reduced survival in patients with gemcitabine-treated pancreas adenocarcinoma. Clin Cancer Res 2004;10:6956–6961.
36. Mohelnikova-Duchonova B, Melichar B. Human equilibrative nucleoside transporter 1 (hENT1): do we really have a new predictive biomarker of chemotherapy outcome in pancreatic cancer patients? Pancreatology 2013;13:558–563.
37. Maréchal R, Bachet JB, Mackey JR, Dalban C, Demetter P, Graham K, Couvelard A, Svrcek M, Bardier-Dupas A, Hammel P, Sauvanet A, Louvet C, Paye F, Rougier P, Penna C, André T, Dumontet C, Cass CE, Jordheim LP, Matera EL, Closset J, Salmon I, Devière J, Emile JF, Van Laethem JL. Levels of gemcitabine transport and metabolism proteins predict survival times of patients treated with gemcitabine for pancreatic adenocarcinoma. Gastroenterology 2012; 143:664–674.e6.
38. Parsons LM, Grzeschik NA, Allott ML, Richardson HE. Lgl/aPKC and Crb regulate the Salvador/Warts/Hippo pathway. Fly (Austin) 2010;4:288–293.

39. Grzeschik NA, Parsons LM, Allott ML, Harvey KF, Richardson HE. Lgl, aPKC, and Crumbs regulate the Salvador/Warts/Hippo pathway through two distinct mechanisms. Curr Biol 2010;20:573–581.
40. Emami KH, Burke TW, Smale ST. Sp1 activation of a TATA-less promoter requires a species-specific interaction involving transcription factor IID. Nucleic Acids Res 1998;26:839–846.
41. Jin X, Pan Y, Wang L, Ma T, Zhang L, Tang AH, Billadeau DD, Wu H, Huang H. Fructose-1,6-bisphosphatase inhibits ERK activation and bypasses gemcitabine resistance in pancreatic cancer by blocking IQGAP1-MAPK interaction. Cancer Res 2017; 77:4328–4341.
42. Su WH, Mruk DD, Wong EW, Lui WY, Cheng CY. Polarity protein complex Scribble/Lgl/Dlg and epithelial cell barriers. Adv Exp Med Biol 2012;763:149–170.
43. Li CH, Xiao Z, Tong JH, To KF, Fang X, Cheng AS, Chen Y. EZH2 coupled with HOTAIR to silence microRNA-34a by the induction of heterochromatin formation in human pancreatic ductal adenocarcinoma. Int J Cancer 2017;140:120–129.
44. Li CH, To KF, Tong JHM, Xiao Z, Xia T, Lai PB, Chow SC, Zhu YX, Chan SL, Marquez VE, Chen Y. Enhancer of Zeste homolog 2 silences microRNA-218 in human pancreatic ductal adenocarcinoma cells by inducing formation of heterochromatin. Gastroenterology 2013; 144:1086.
45. Chen Y, Lin MC, Yao H, Wang H, Zhang AQ, Yu J, Hui CK, Lau GK, He ML, Sung J, Kung HF. Lentivirus-mediated RNA interference targeting enhancer of zeste homolog 2 inhibits hepatocellular carcinoma growth through down-regulation of stathmin. Hepatology 2007; 46:200–208.
46. Arao T, Yanagihara K, Takigahira M, Takeda M, Koizumi F, Shiratori Y, Nishio K. ZD6474 inhibits tumor growth and intraperitoneal dissemination in a highly metastatic orthotopic gastric cancer model. Int J Cancer 2006;118:483–489.
47. Zhang G, Schetter A, He P, Funamizu N, Gaedcke J, Ghadimi BM, Ried T, Hassan R, Yfantis HG, Lee DH, Lacy C, Maitra A, Hanna N, Alexander HR, Hussain SP. DPEP1 inhibits tumor cell invasiveness, enhances chemosensitivity and predicts clinical outcome in pancreatic ductal adenocarcinoma. PLoS One 2012;7:e31507.

Received March 13, 2020. Accepted June 22, 2020.

Correspondence
Address correspondence to: Yangchao Chen, PhD, School of Biomedical Sciences, Faculty of Medicine, Chinese University of Hong Kong, Shatin, Hong Kong. e-mail: yangchaochen@cuhk.edu.hk; fax: (852) 26035123.

CRediT Authorship Contributions
Yin-Xin Zhu, PhD (Data curation: Lead; Formal analysis: Lead; Investigation: Lead; Methodology: Lead; Writing – original draft: Lead); Chi Han Li, PhD (Data curation: Supporting; Formal analysis: Supporting; Writing – review & editing: Supporting); Guolin Li (Data curation: Supporting; Formal analysis: Supporting); Huiyi Feng (Data curation: Supporting; Formal analysis: Supporting); Tian Xia (Data curation: Supporting); Chi Hin Wong (Data curation: Supporting); Frederic K. C. Fung (Data curation: Supporting); Joanna Hung Man Tong (Data curation: Supporting); Ka-Fai To (Data curation: Supporting); Yangchao Chen, PhD (Conceptualization: Lead; Funding acquisition: Lead; Investigation: Supporting; Project administration: Lead; Resources: Lead; Supervision: Lead; Validation: Lead; Writing – review & editing: Lead); Rufu Chen (Data curation: Supporting).

Conflicts of interest
The authors disclose no conflicts.

Funding
Supported by grants from the National Natural Science Foundation of China (81672323), the General Research Fund, Research Grants Council of Hong Kong (14171217 and 14120618), and a direct grant from The Chinese University of Hong Kong (Y.C.).